electronics

MDPI

Article

Tools for Researching the Parameters of Photovoltaic Modules

Milan Belik [1,2], Oleksandr Rubanenko [3], Iryna Hunko [3,4], Olena Rubanenko [3,4,5], Serhii Baraban [6,*] and Andriy Semenov [7]

1 Department of Electrical Power Engineering, Faculty of Electrical Engineering, University of West Bohemia, 30614 Pilsen, Czech Republic; belik4@fel.zcu.cz or belik@cefas.cz
2 Department of Simulation RES, Czech Photovoltaic Association, z.s., Teslova 1202/3, 30100 Pilsen, Czech Republic
3 Department of Power Plants and System, Vinnytsia National Technical University, 21021 Vinnytsia, Ukraine; rubanenkoae@ukr.net (O.R.); iryna_hunko@vntu.edu.ua (I.H.); olenarubanenko@ukr.net or rubanenk@fel.zcu.cz (O.R.)
4 Department of Wind Power, Institute of Renewable Energy, 02094 Kyiv, Ukraine
5 Research and Innovation Center for Electrical Engineering (RICE), Faculty of Electrical Engineering, University of West Bohemia, 30614 Pilsen, Czech Republic
6 Faculty of Computing and Telecommunications, Poznan University of Technology, 60965 Poznan, Poland
7 Faculty of Information Electronic Systems, Vinnytsia National Technical University, 21021 Vinnytsia, Ukraine; semenov.a.o@vntu.edu.ua
* Correspondence: serhii.baraban@put.poznan.pl; Tel.: +48-515179906

Abstract: This paper addresses critical challenges in renewable energy research, particularly under the difficult operational conditions caused by the military conflict in Ukraine. Despite significant infrastructure loss due to the armed conflict (13% of solar and 70% of wind power), Ukraine maintains a commitment to reach 27% renewable energy in final consumption by 2030. However, the wartime conditions present unique challenges to scientific research, with laboratories vulnerable to missile strikes and frequently requiring evacuation. This paper introduces innovative portable laboratory stands designed for comprehensive analysis and monitoring of photovoltaic (PV) module parameters. These portable platforms, integrating advanced microcontrollers, sensors, and data-processing units, enable effective real-time monitoring and parameter estimation of PV modules, thereby enhancing their operational efficiency and reliability. Two distinct portable laboratory setups were developed and are detailed: the first focuses on real-time voltage and current measurements, while the second, termed the photovoltaic module parameter scanner (SPFEM), emphasizes data collection, remote data transmission, and database integration for subsequent analysis. This research provides essential tools for ensuring continuity in scientific activities and practical training for students and researchers amidst the ongoing security threats. The presented systems significantly contribute to optimizing the performance of PV systems in Ukraine and underscore the necessity for continuous adaptation and technological advancement in renewable energy infrastructure.

Keywords: photovoltaic modules; portable and mobile laboratory stands; scanner of parameters of photovoltaic modules; renewable energy

check for updates

Academic Editor: Rui Castro

Received: 3 April 2025
Revised: 27 April 2025
Accepted: 30 April 2025
Published: 6 May 2025

Citation: Belik, M.; Rubanenko, O.; Hunko, I.; Rubanenko, O.; Baraban, S.; Semenov, A. Tools for Researching the Parameters of Photovoltaic Modules. *Electronics* **2025**, *14*, 1885. https://doi.org/10.3390/electronics14091885

Copyright: © 2025 by the authors. Licensee MDPI, Basel, Switzerland. This article is an open access article distributed under the terms and conditions of the Creative Commons Attribution (CC BY) license (https://creativecommons.org/licenses/by/4.0/).

1. Introduction

The last decade up to the present day has been marked by the ongoing impact of pandemics (such as COVID-19), active military operations, the mass destruction of educational and research facilities, and the loss of teachers, students, and researchers. The time spent in modern classrooms and existing research institutions is decreasing. The time spent in bomb shelters and shelters is increasing.

At the same time, the motivation to maintain high quality in the educational process and to train highly qualified specialists, especially in the current conditions, encourages us to seek and find new ways, methods, and means of ensuring high-quality education and research activities in conditions of frequent use of CBRN (chemical, biological, radiological, and nuclear) weapons, periodic shelling with hypersonic missiles, strike drones, etc.

Today, the cost of fossil fuels is steadily rising. Therefore, the cost of electricity generated by power plants is also increasing. It is important to improve the methods and means of reliable electricity generation using solar, hydro, wind, etc., energy and methods of transmitting this electricity from its source (power plant) to consumers [1,2]. The installed capacity level of photovoltaic power plants has increased in the last ten years in Ukraine. The IRENA's report presents the energy profile for Ukraine (Figure 1):

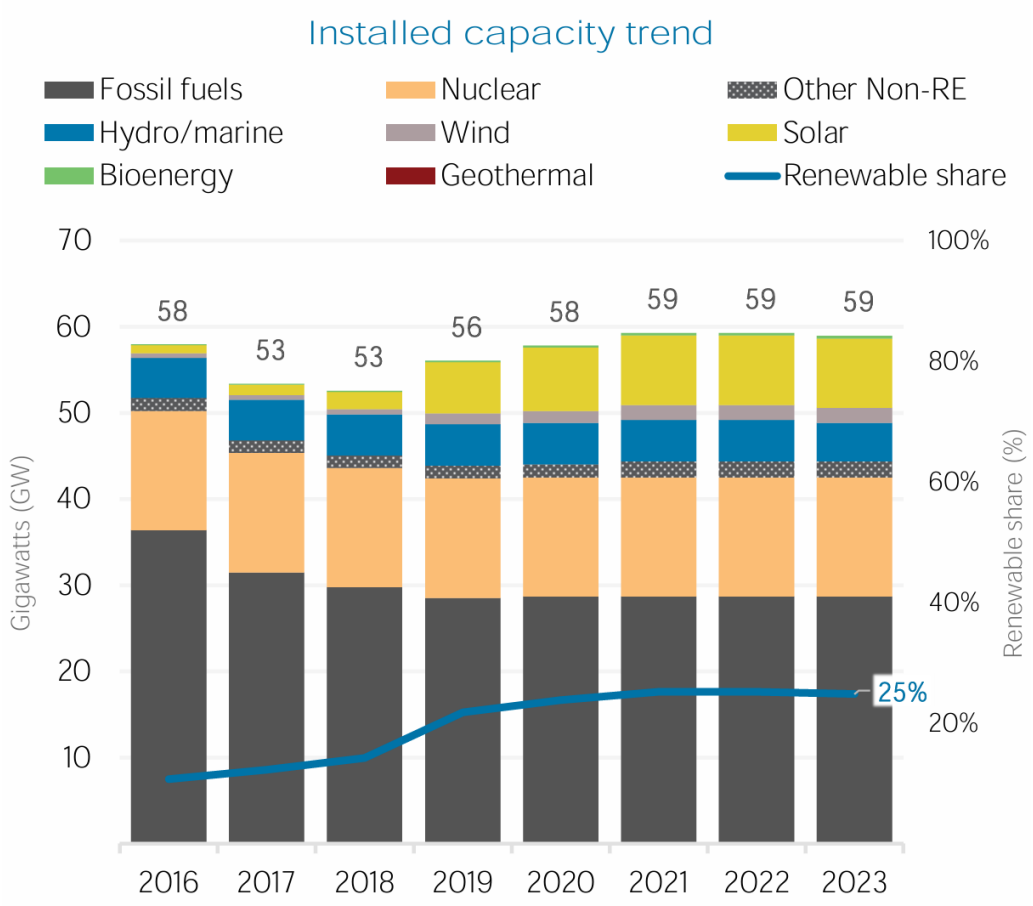


Figure 1. Energy profile for Ukraine.

In the DIXI group report, it is noted that, despite the significant loss of capacity due to the occupation (13% of solar and 70% of wind power), the sector continues to demonstrate a course of recovery and modernization. According to the targets approved at international level by the Ministerial Council of the Energy Community, by 2030 the share of renewables in final energy consumption should reach 27%, with the expected largest contribution being to electricity consumption [3].

The Europe Action Plan for Ukraine, "Resilience, Recovery, and Reconstruction" 2023–2026, notes the development and delivery of specialized training courses on topics relevant to investigations of the energy sector/supervisory control and data acquisition (SCADA), open source intelligence (OSINT), and others. The National Renewable Energy Action Plan for Ukraine aims to increase the share of renewable energy to 27.1% of the total gross energy consumption by 2030. The main goals for Ukraine, as a member of the EU, are

as follows: deploying more renewable energy, saving energy, and diversifying its energy supplies. Furthermore, the EU has agreed on stronger legislation to increase its renewable capacity by raising its binding target for 2030 to a minimum of 42%, effectively doubling the existing share of renewable energy in the EU. Implementing this policy requires high-quality personnel, particularly in power engineering for renewable energy. This requires modern scientific laboratories, equipment, and laboratory stands where scientists (masters, graduate students, doctoral students, and researchers) can conduct research, test hypotheses, develop new solutions, and obtain new patterns. The problem of conducting scientific research in Ukraine is the rocket attacks on cities and critical infrastructure enterprises (power plants and substations) (Figure 2) [4–8].



Figure 2. Damage to the photovoltaic modules at the solar power plant as a result of missile strike.

The Ukrainian war energy crisis has shown that the energy sector needs significant modernization to reach energy safety and achieve the Green Deal objectives. This modernization of the energy sector is fundamentally dependent on capacity building in higher education institutions (HEIs).

Research laboratories located in the area of possible missile and guided bomb hits require frequent interruptions of research and evacuation of researchers to bomb shelters.

Wartime conditions in Ukraine have severely impacted the energy sector and research infrastructure. Frequent missile attacks on cities and power plants (Figure 2) interrupt grid power and make conventional laboratories unsafe. This wartime energy crisis underscores the need for resilient, decentralized solutions to maintain critical services. For example, off-grid solar installations have been deployed to restore electricity in conflict zones: more than half of households in Yemen now rely on solar lighting amid grid collapse, and similar renewable energy deployments in Syria and Ukraine have provided essential power to hospitals and military outposts. These cases motivated our work: developing portable PV module research stands that allow engineers and students to continue experimentation and monitoring even as fixed labs are compromised by war.

In addition to addressing the urgent local energy challenges caused by the conflict in Ukraine, the development of portable renewable energy solutions aligns with global trends and international efforts aimed at enhancing energy resilience and sustainability. The following sections briefly summarize the global significance and key benefits of renewable energy and mobile laboratory systems.

Renewable energy is crucial for addressing global environmental issues and ensuring sustainable energy development. It plays a significant role in reducing greenhouse gas emissions and mitigating climate change [9,10]. Renewable energy sources, such as solar, wind, hydropower, geothermal, and biomass, are abundant and can meet global energy demands multiple times over [9]. These sources are essential for the transition away from fossil fuels, which are finite and contribute to environmental degradation [11].

Renewable energy technologies offer a wide range of critical advantages that extend beyond environmental protection. Firstly, by significantly reducing emissions of greenhouse gases and air pollutants, renewable sources contribute to cleaner air quality and mitigation of the effects of climate change [10,12]. In addition to environmental benefits, renewable energy drives local and regional economic development by creating new employment opportunities and improving access to affordable energy, particularly in underserved and developing areas [12,13]. In addition, the widespread adoption of renewables strengthens global energy security by reducing dependence on volatile fossil fuel markets [14]. Finally, since renewable resources such as solar, wind, and hydro are naturally replenished they provide a sustainable foundation to meet long-term energy demands without exhausting finite natural resources [11].

Mobile laboratory systems play an increasingly vital role across the education, research, healthcare, and emergency-response sectors. By enabling flexible, on-site diagnostics and experimentation, mobile laboratories expand access to critical scientific tools and capabilities, particularly in remote, conflict-affected, or underserved regions [15,16]. Their ability to deliver laboratory-grade functions directly to the field addresses infrastructure challenges and enhances resilience in environments where traditional facilities may be limited or inaccessible.

Mobile laboratories provide a diverse range of societal and technological benefits: Firstly, they significantly enhance educational outreach by offering hands-on science and engineering education, bringing advanced instrumentation and experimental experiences to students who might otherwise lack access [16]. Secondly, they are indispensable in emergency-response operations, where rapid deployment of diagnostic tools is essential for managing disease outbreaks, environmental disasters, and humanitarian crises [15,17]. Finally, mobile laboratories facilitate research and development by allowing technologies and methodologies to be evaluated directly under real-world conditions, accelerating innovation cycles and promoting practical application [18,19].

The purpose of this article was to develop and implement program and multidisciplinary portable laboratory stands for studying disciplines related to renewable energy and automation systems. To achieve this goal, the following tasks were achieved:

1. We analyzed the current situation on the state of renewable energy sources in Ukraine.
2. We analyzed the existing problems with practical and laboratory work for students of energy specialties and develop ways to solve them.
3. The configuration of two laboratory stands was proposed to conduct classes in disciplines related to the management of photovoltaic stations.
4. The interface and software of the proposed laboratory stands were developed and improved.

Interesting articles on the studied topic from well-known databases (IEEE, Springer, etc.) were analyzed. The photovoltaic power plant is a complex system and requires deep research. The strategic research directions for PV energy generation under wartime and decentralized conditions are summarized in Figure 3.

The authors present research on PV module degradation, with a table illustrating more attention to early PV module failures [20]. The results of the presented study can be implemented for the identification of photovoltaic system malfunctions under Ukrainian conditions. For example, studying the influence of the processing conditions of encapsulation on the degradation mechanisms of solar cells in the first year is important [20], because this problem appears in the Ukrainian photovoltaic power plant [21]. Accurate knowledge of the parameters of the PV module model is crucial for optimizing PV power-generation systems, and this study introduces the single-diode model [22], analyzes the influence of the parameters on the characteristics of the iV, and employs various algorithms to estimate the parameters' values,

highlighting the complexities and sensitivities involved. The PV hotspot fault detection model was presented in paper [23], and it is a network based on region perception and aggregation of features across channels, which can be studied on data collected from Ukrainian PV power plants. In paper [24], an analysis was presented that revealed the optimal inclination angles of the photovoltaic system for the housing, public, service, and manufacturing sectors. This idea is realized in the laboratory stand. Papers [25–27] showed the diagnostic methods of the PV system, tools, and methodologies for researching and studying the parameters (open-circuit voltage (*Voc*); short-circuit current (*Isc*); maximum power point (*MPP*); fill factor (*FF*), etc.). Photovoltaic modules should be available to students. The evaluation of the effectiveness of the photovoltaic system and the defense of the ways in which energy generation can be optimized are presented in the next paragraph.

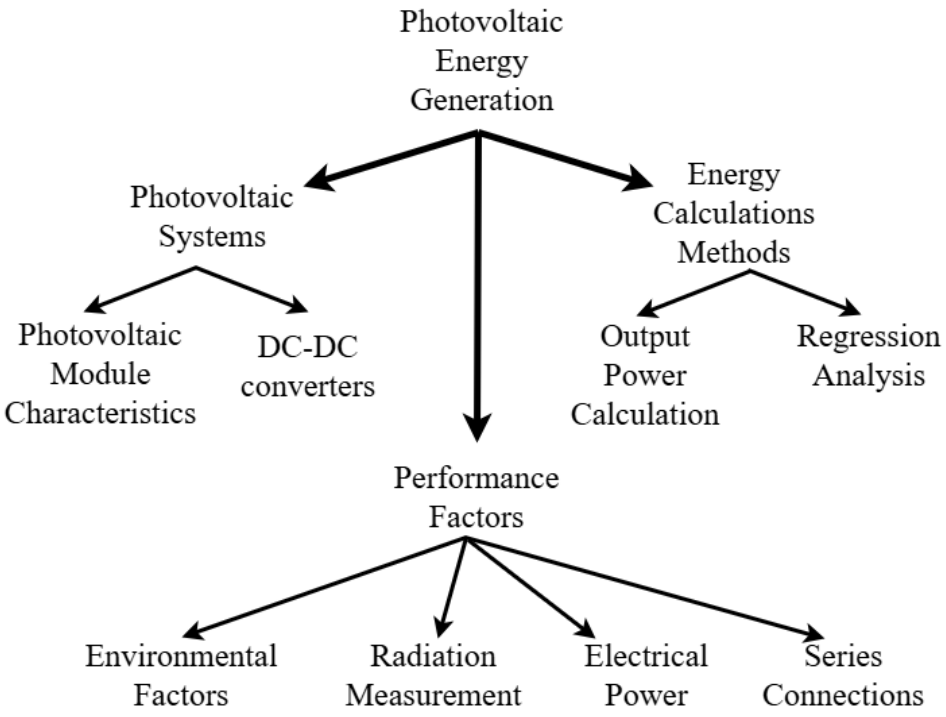


Figure 3. Research direction of the PV energy generation.

The novelty of our approach lies in a portable, self-contained design that integrates advanced microcontrollers and sensors to maintain research capabilities despite conflict-related evacuations. Unlike commercial PV test labs, which are large and stationary, our two proposed systems can be quickly deployed or transported, enabling real-time PV module analysis in field conditions where traditional labs are unavailable. These superior features (compactness, remote data logging, and operation on limited power) make the systems especially suitable for war-damaged environments and educational use in crisis, bridging a critical gap in existing solar PV diagnostic tools.

The main advantages are low cost, the possibility of improvement, and that the controllers are selected so that new sensors can be added over time. Another advantage of the proposed stands is their mobility and ease of transportation. In addition to the characteristics and parameters of photovoltaic systems that can be studied on conventional laboratory stands, it is proposed to study the radiation frequency and the location of the radiation source in order to compensate for shading. Another difference is the control of the tracker (i.e., changing the angle of the photovoltaic panel) depending on the wind strength.

This research addresses significant gaps identified in the current literature. Specifically, we bridge the methodological gap by introducing innovative portable laboratory setups

explicitly designed for renewable energy research under challenging wartime conditions, a scenario overlooked by conventional stationary systems. We also fill an empirical gap by providing practical data and validation for the performance and resilience of these mobile laboratories in operational conflict environments—an aspect not sufficiently explored in prior studies. Lastly, this work addresses a knowledge gap through detailed examination of photovoltaic modules' behavior under varying shading conditions and LED backlighting frequencies. Addressing these gaps, this paper contributes novel insights and practical methodologies critical to the advancement of renewable energy research and education amidst crisis conditions.

The original contributions of this work are as follows:

(1) Development of two novel, low-cost, portable laboratory systems specifically designed for photovoltaic module diagnostics under wartime and emergency conditions;
(2) Practical validation of the systems' portability, robustness, and operational performance in simulated conflict-affected environments;
(3) Empirical analysis of shading effects and LED illumination frequency impacts on PV module performance, with implications for maintaining renewable energy systems in disrupted grid conditions;
(4) Provision of an open source, modular approach (including hardware schematics and software) to facilitate rapid replication, deployment, and scalability of portable photovoltaic testing setups across institutions facing infrastructure instability.

2. Materials and Methods

2.1. PV System Efficiency Calculation

Increasing the energy generation of the PV system requires more precise control of the technical conditions and choosing the correct type of PV module [27–29]. The efficiency of the PV system can be determined as the ratio of the daily energy generation $E_{AC,D}$ (kWh) and the daily solar radiation H_t (kWh/m^2) reaching the surface of the PV module times the area of the PV system (in our case, it is one area of the PV module) in (m^2) [30]

$$\eta = (\frac{E_{AC,D}}{H_t \cdot A_S}) \cdot 100, \quad (1)$$

$$E = A_s \cdot r \cdot H_t \cdot PR \cdot h, \quad (2)$$

In Equation (2), r means solar panel yeld (%); PR is the performance ratio, the index to take losses into account (which can change from 0.9 up to 0.5); and h is the number of hours of the study period. To minimize the deviation between the real and calculated values, efficiency and energy need to take into account the specific conditions of operation of the photovoltaic power plant, including the frequency of the energy sources or biological corrosion of the panels. The influence of this corrosion can be different, depending on the orientation of the PV modules, the location of the design cells, and the distance between the frame and the cell. In this case, Equations (1) and (2) can be rewritten:

$$\eta = (\frac{E_{AC,D}}{H_t \cdot A_{pv_mod_usefull}}) \cdot 100, \quad (3)$$

$$E = A_{pv_mod_usefull} \cdot r \cdot H_t \cdot PR \cdot h, \quad (4)$$

$$A_{pv_mod_usefull} = A_{pv_mod_cor}, \quad (5)$$

where $A_{pv_mod_cor}$ is the area of the PV module that is not available, due to biological corrosion; A_{pv_mod} is the complete area of the PV module.

For detailed analyses of efficiency photovoltaic modules, portable test benches have been developed and are presented in the following paragraphs. A stand has been developed to analyze the efficiency of a photovoltaic module, depending on the changing frequency of the source.

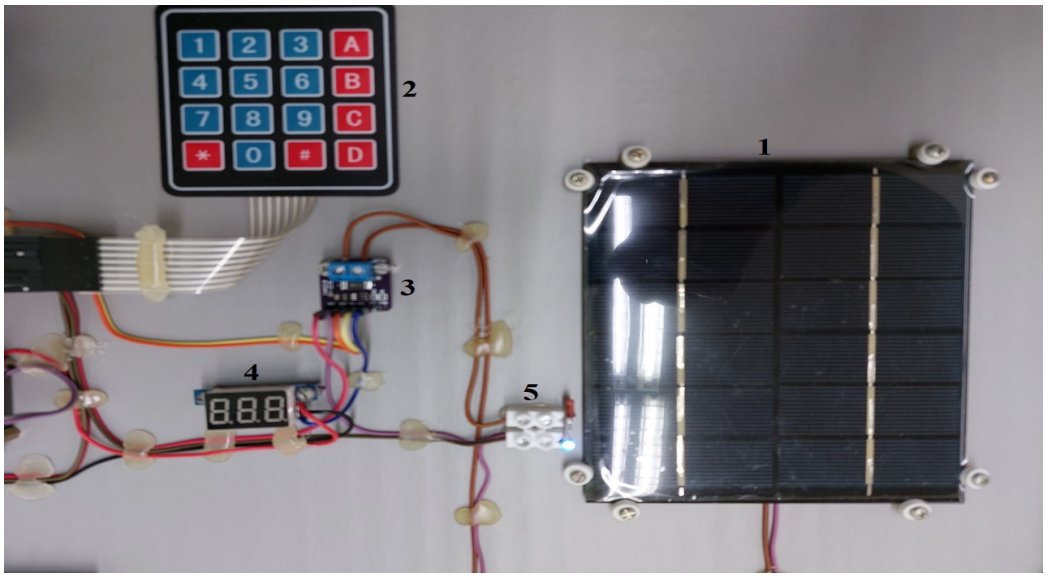
2.2. Portable Test Bench for Studying the Parameters of Photovoltaic Modules

Let us consider portable stand 1 for controlling and studying the parameters of photovoltaic modules. Figure 4 shows fragments of stand 1. Figure 4a shows a photovoltaic panel. Figure 4b,c show the Arduino Uno board from Arduino, built on the ATmega 328 microcontroller (Microchip Technology Inc., Chandler, AZ, USA). The ATmega328 has flash, SRAM, and EEPROM memory, namely, FLASH—32 kB, of which 0.5 kB is used to store the bootloader, SRAM—2 kB, and EEPROM—1 kB (acessible via the EEPROM library).

The serial interface is used for control. The control of indicators and the detection of button presses is performed by the TM1638 chip from from Titan Microelectronics Co., Ltd. (Chengdu, China). TM1638 receives from the MC and transmits data through a unique serial interface of three signals, close to the SPI interface. The difference from SPI is the combination of two lines of reception and transmission in one line. The signal names are different from those used in SPI, but they are well recognized.

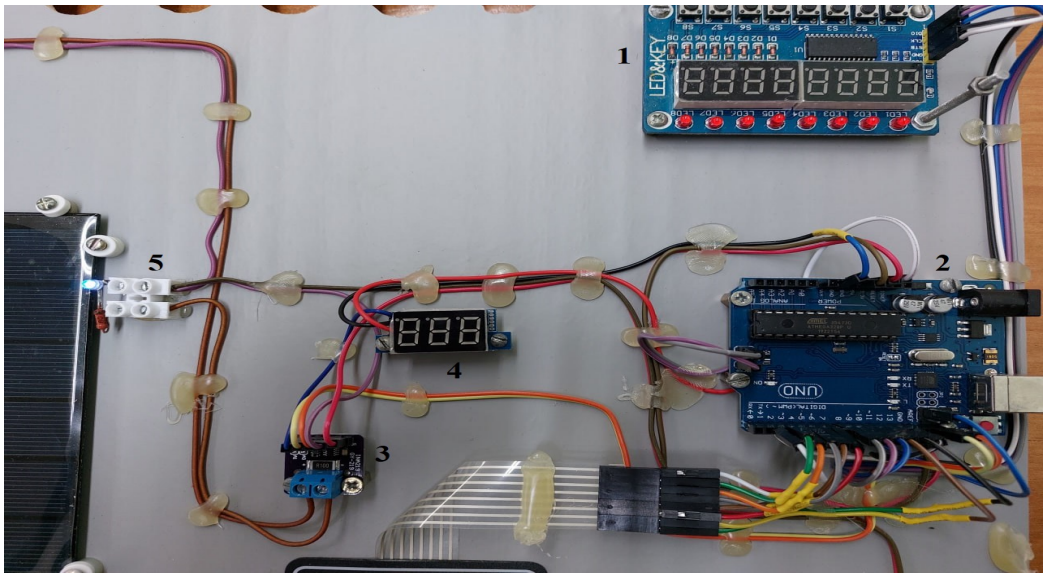
There is also a voltmeter board that allows one to determine the DC voltage at the output of the photovoltaic panel and transmits the measured voltage signal to a three-digit display with three seven-segment indicators.

Secondly, stand 2—the scanner of the photovoltaic module (SPPVM) parameters is shown in Figure 5. The appearance of the SPFEM tested board is shown in Figure 6.

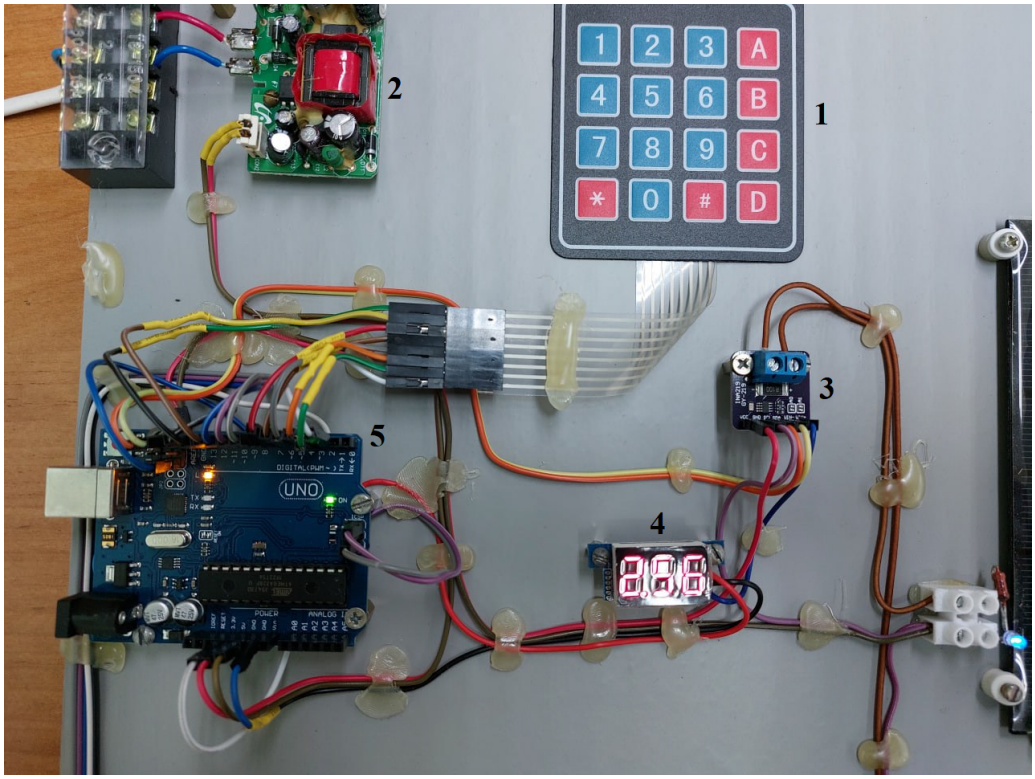


(**a**)

Figure 4. *Cont.*



(**b**)



(**c**)

Figure 4. Test bench for control and research of the photovoltaic module: (**a**) 1—small PV module, 2—4 × 4 matrix membrane keypad, 3—voltage converter module, 4—TM1637 4-digit 7-segment display module, 5—screw terminal block connector; (**b**) 1—TM1638 module, 2—Arduino UNO board, 3—voltage converter module, 4—TM1637 4-digit 7-segment display module, 5—screw terminal block connector; (**c**) 1—4 × 4 matrix membrane keypad, 2—DC–DC buck converter module, 3—voltage converter module, 4—TM1637 4-digit 7-segment display module, 5—Arduino UNO board.



Figure 5. Scanner of parameters of photovoltaic module: 1—SPPVM body, 2—C1, C2, C3 connectors for connecting current, voltage, and temperature sensors of the photoelectric module, 3—LED indicator of SPPVM operating mode: (LED off—SPPVM is disabled, LED on—SPPVM is enabled, LED flashing—SPPVM is transmitting data).

SPFEM is a mobile device that can work as part of a combination of devices and can perform the tasks of collecting PV module parameters, transferring the collected data to a laptop or to a remotely located server, automatically generating a database and saving this database to a Google disk.

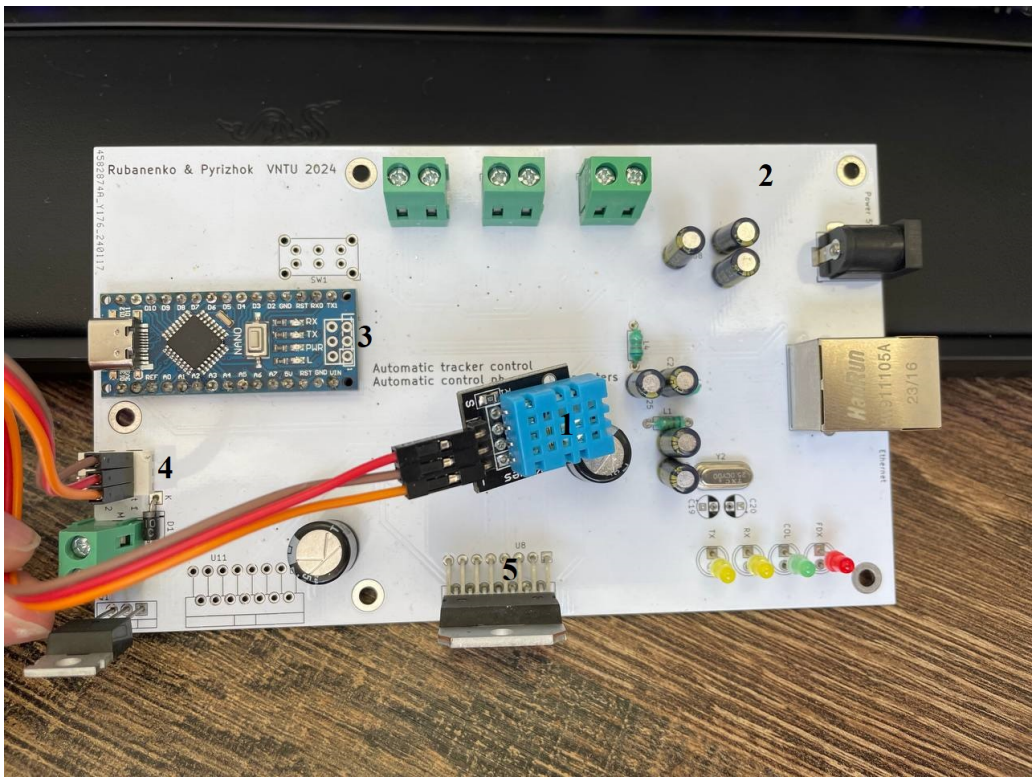


Figure 6. The view of the SPFEM testbed board: 1—DHT11 sensor module, 2—Arduino Nano development board, 3—Arduin Nano, 4—dupont wires, 5—voltage regulator IC.

It allows you to use a notebook to program the ATMega328p microcontroller (change the program code) on the Arduino uno board and use this controller to obtain information about the electrical energy generated by the photovoltaic panel, the voltage and current of the photovoltaic module. Using the ATmega 16U2 communication controller (Microchip Technology Inc., Chandler, AZ, USA), the research bench is connected to a laptop. The developed programs allow us to accumulate the results of observations and store these results in the form of databases on a specially created server and on Google disk. Observation re-

sults can be retrieved, viewed, and processed. These results can be converted and presented in the form of MS Excel files.

2.3. Block Diagram of the System for Monitoring the Parameters of the PV System

A graphical representation of the parts of the PV module parameter monitoring system that are interconnected by a certain feature and ways of action transmission is called a system block diagram.

The system for monitoring the parameters of photovoltaic modules consists of two main blocks (Figure 7), such as a device based on the ATmega328P microcontroller (Figure 8) and a data-processing server (Figure 9).

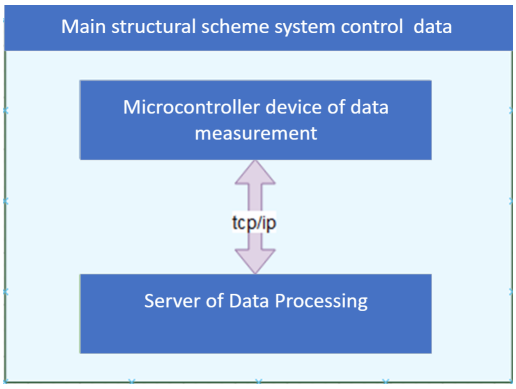


Figure 7. Main structural scheme of the system for monitoring the parameters of photovoltaic modules.

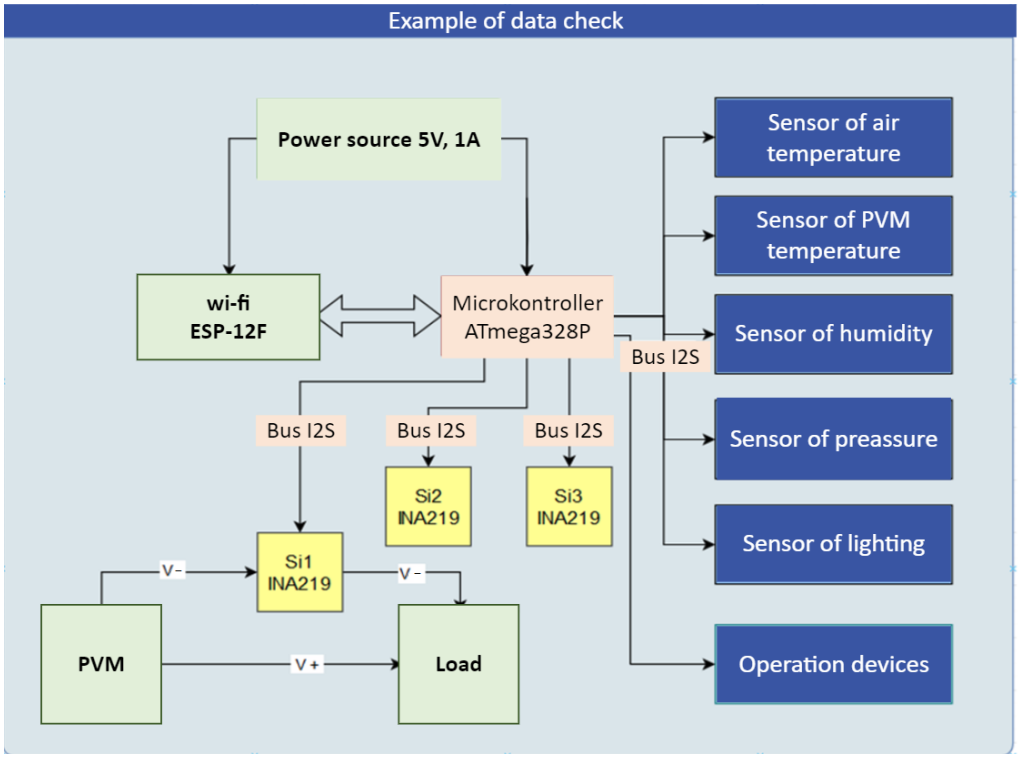


Figure 8. Structural scheme of the system for monitoring the parameters of photovoltaic modules.

These sensors record the voltage, current, and power of the load connected to the PV system and transmit the parameters received to the microcontroller at a specified frequency. In the Figure 9 block, INA 219 is shown:

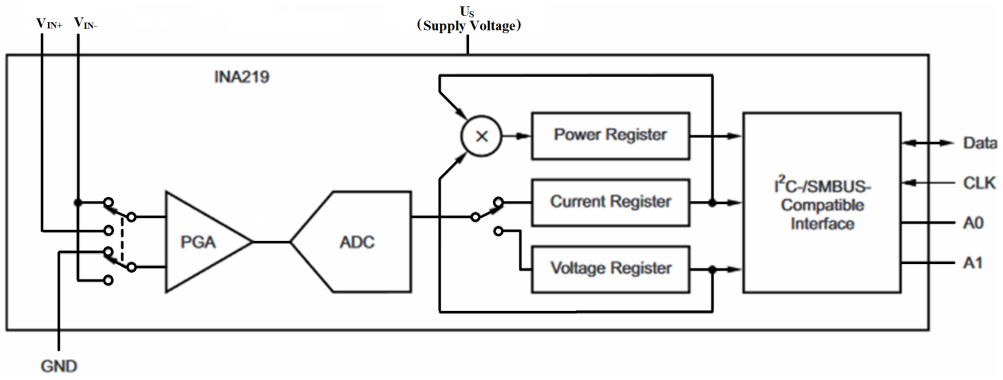


Figure 9. Block INA 219.

The choice of the Arduino Uno board (ATmega328 microcontroller) was specifically driven by its widespread availability, affordability (typically under $20), and ease of use, critical during wartime disruptions when supply chains and financial resources are severely constrained. This microcontroller is popular, well supported by a vast community, and extensively documented, making troubleshooting and replacement significantly simpler under challenging conditions. Furthermore, the Arduino Uno operates reliably at low power (5 V via USB or small batteries), making it suitable for field use without access to stable electricity.

Sensor modules, such as the TM1638 (control/display module), INA219 (voltage/current sensor), and other peripheral components were also selected based on their affordability, robustness, and common availability on international and local markets, even under wartime conditions. Importantly, these sensors require minimal calibration, provide adequate accuracy (2–3%), and can be easily replaced if original parts become unavailable due to interrupted supply chains. Thus, the chosen components balance cost effectiveness, ease of replacement, and robustness—factors that are vital in an uncertain and resource-constrained wartime operational environment.

In addition, using the appropriate sensors, the microcontroller receives data such as the temperature of the ambient air around the photovoltaic module, the temperature of the PV module itself, air humidity, air pressure, and the intensity of the light on the photopanel. It is also possible to connect various actuators to the controller, such as motors, stepper motors, pumps, relays, etc. In addition, the product is equipped with the necessary LED indication. This device is equipped with a WI-FI module, through which the microcontroller communicates with the data-processing server via the TCP/IP protocol. The microcontroller operates with the help of programmed software written in the C language. The data-processing server—the Cisco UCS C240 M5—is a rackmount server that belongs to high-performance server equipment. The system runs on the Debian 12 operating system. To run the software on the server, it is necessary to install PHP version 7.2 or higher, MySQL database, and Apach Web server. The software of the PV system consists of a visual part in the form of an HTML page that works in any browser (frontend), written in JavaScript(ECMAScript 2020 standard), compatible with modern browsers such as Google Chrome Version 123.0.6312.105 and API (mechanisms that allow two software components to interact with each other using a set of definitions and protocols), and written in PHP Version 7.4 as the backend. In addition, the software of the PV control system includes a database (MySQL) that accumulates and stores data from the controller, as well as all the parameters and modes necessary for the system operation. The system starts by setting up a wireless WI-FI network on the device of the PV parameter monitoring system and connecting it to the data-processing server. After that, the controller modes are set, such as automatic/manual, the time of the interval for receiving data from sensors in automatic mode, and others. The device then switches to operating mode and starts collecting data from

the PV modules and the external environment, transferring these data to the data-processing and storage server. When certain data, such as the temperature of the solar cell, reaches thresholds, the microcontroller, according to a programmed algorithm, begins to perform certain actions, such as activating certain actuators to cool the solar cell. When the temperature of the PVM decreases, the microcontroller deactivates the actuators and stops cooling the solar cell. The visualization of the PVM control system is presented in Figure 10.

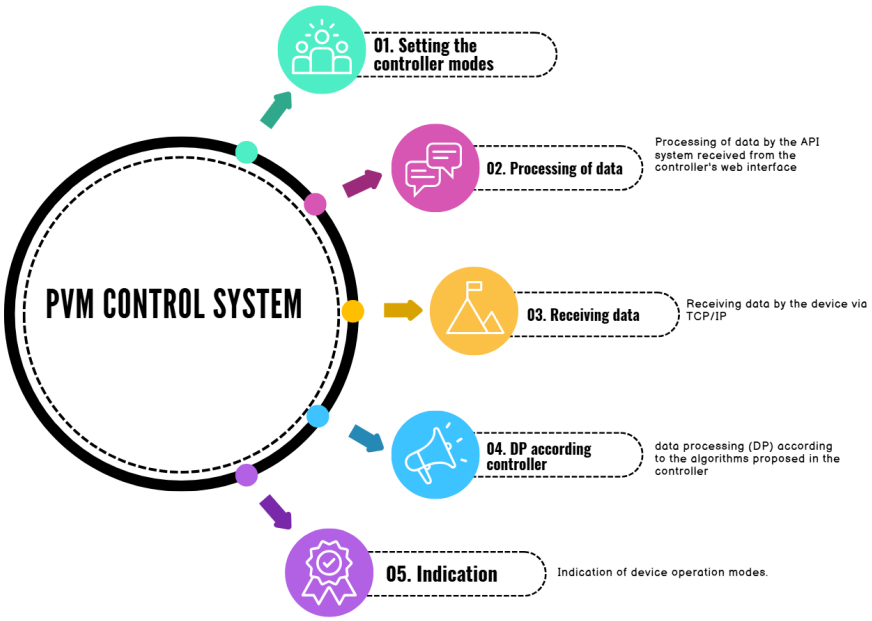


Figure 10. PVM control system.

2.4. PVMCS Testbed Program Code for Controlling the Panel Generation Parameters

First, the portable PV test bench was connected to the PV module placed outdoors under clear-sky conditions, typically around midday (11:00–14:00 local time) to maintain approximately stable irradiance (950–1000 W/m²). Ambient temperatures ranged from 20 °C to 25 °C. The Arduino-based data-acquisition system was initialized and the sensors were calibrated against standard multimeters prior to each test. Measurements were taken continuously for intervals of 10–15 min at each location, recording voltage, current, and temperature every minute. Special attention was paid to avoiding direct solar exposure of electronic modules, employing protective shading where necessary to simulate realistic field conditions encountered during wartime operations.

The program code is written in the C programming language using the Arduino IDE Version 1.8.19, in combination with the ESP8266 board support package Version 3.1.2.

To run the program, the controller connects libraries such as Arduino.h to work with the EEPROM memory chip, the EEPROM.h library. To operate the ESP8266WiFi module, the ESP8266WiFi.h and ESP8266HTTPClient.h libraries are used. At the beginning of the program, all the constants necessary for the device operation are set: the microcontroller pins to which the LED indication is connected, the name and password of the wireless WI-FI network for access to the internet, the domain address of the server where the API for working with the device is located, and others. After that, the device's non-volatile EEPROM memory is worked with, and all the necessary data for the program are read and written in the for loop. The program is initialized in the void setup() function. First, the necessary controller outputs are programmed to the OUTPUT mode, after which their logic level (LOW) is set and a delay of 0.1 s is set. The next step is to read all the

necessary data from the EEPROM to connect to the WI-FI network, and then to write the connection itself.

The main algorithm and the program cycle are in the void loop function. In this loop, the program interrogates the data of the sensors connected to them from the programmed ports of the controller at a given interval, generates the necessary data, and sends them to the server for processing and storage via the http protocol. The text of the program is presented in Appendix A.

2.5. A Stand for Researching the Tracker Parameters of a Photovoltaic Station

Another portable stand is a stand for studying tracker parameters (Figure 11). Control panel 5 has two buttons and a variable resistor. The first button changes the tracker control mode from manual control to automatic control of the movement of the tracker desktop. The second button changes the possibilities of manual control of the position of the tracker desktop: position control from left to right, and from top to bottom. The control itself is carried out using the rod of the variable resistor located on control panel 5. The direction of movement of desktop 2 is changed by changing the direction of movement of the rod of the variable resistor on control panel 5 in manual mode. In automatic mode, the tracker desktop 2 moves automatically, following the movement of the light source.

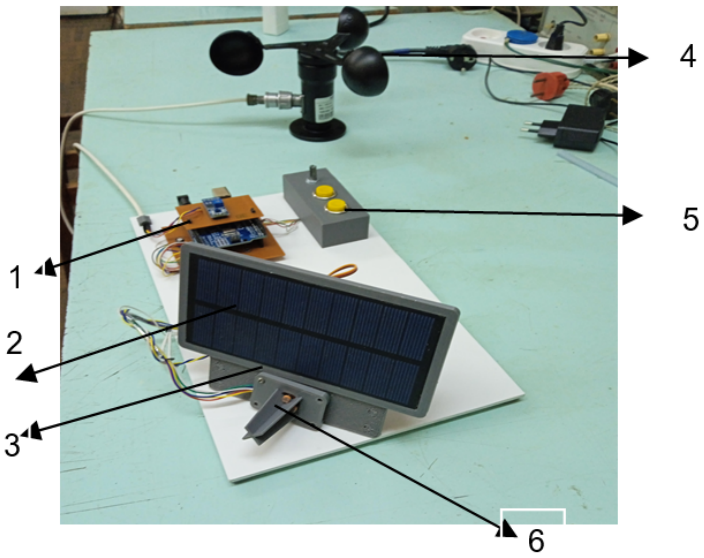


Figure 11. Stand for researching tracker parameters: (1) control circuit and microcontroller, (2) tracker desktop (photovoltavic panel), (3) servo mounting mechanism, (4) anemometer, (5) control panel with buttons and variable resistor, (6) baseboard.

Figure 11 illustrates the assembled experimental stand used for analyzing solar tracker performance under variable lighting conditions. The setup integrates multiple modules, including an Arduino Uno controller, a tracker platform equipped with a photovoltaic panel, and a control interface. Additional components include an anemometer for potential wind-speed compensation, and a photodiode module for directional light sensing.

The tracker setup experiments were performed indoors in a controlled laboratory environment to ensure consistent conditions. A standard desk lamp with adjustable positioning simulated the solar source. The tests began by manually aligning the tracker, followed by switching to automatic mode. The response of the tracker was evaluated by systematically moving the lamp source horizontally and vertically. The tracker response times (1–3 s), positional accuracy, and corresponding photovoltaic output were recorded. The ambient laboratory temperatures during these tests remained stable around 22 °C ± 1 °C, avoiding

significant temperature-induced measurement variations. Robustness against external disturbances (e.g., simulated wind conditions) was evaluated by manually introducing brief controlled vibrations into the set-up.

The program code, which is stored in the Flash memory of the Atmel processor on the Arduino Uno board, is shown later in the text of the article in Appendix B. This code not only allows you to control the parameters of the photovoltaic panel, but also controls the wind speed. If the wind speed exceeds the set point, the Arduino Uno board gives a command to change the position of the desktop from the current position to a horizontal position.

2.6. Investigation of the Influence of the Frequency of LED Backlighting of a Photovoltaic Panel on Its Photocurrent

Tests evaluating the effect of LED illumination frequency on PV panel photocurrent were performed in a darkened laboratory room to eliminate extraneous ambient lighting effects. A calibrated white LED was placed at a fixed distance (approximately 15 cm) from the surface of the photovoltaic module, delivering consistent peak illumination (5000 lux measured with a calibrated luxmeter). The illumination frequency was systematically varied from 20 Hz to 220 Hz, using a controlled function generator, with a fixed duty cycle of 50%. The photocurrent was measured with an INA219 sensor module integrated with the portable test bench, recording data points at each frequency step over a 10 s interval, ensuring the stabilization of the readings. Throughout the experiments, room temperature was maintained consistently at 22 °C ± 1 °C to avoid thermal influence on panel performance measurements.

The task arose to temporarily increase photovoltaic generation in order to level the daily PV generation schedule. It is necessary to investigate whether the photocurrent (variable y) generated by the solar cell (measured in microamperes) depends on the frequency (factor x—measured in hertz). For this purpose, ANOVA analyses can be used [20,21]. Let us assume that the assumptions of the variance analysis are met—that is, the PV current has a normal distribution and the backlight frequency has no effect on the variance σ_2 of y, but causes a divergence of the mean values. We selected frequency groups that were fed to the photovoltaic panel of a series of samples from six batches (batch number j varied from 1 to u) of products (u = 4). The number of measurements in each batch l varied from 1 to 5 (m). The results of the measurements and the division into groups are shown in Table 1. The calculations in the same table are self-explanatory and were necessary to find the sum of the squared deviations and sample variances: $y_{1,1} = 10$ mA; $y_{1,2} = 10.0$ mA; $y_{1,3} = 10.3$ mA; ... $y_{4,5} = 7.8$ mA, etc. From each batch of lamps, we took the first measurement result and found the sum of the first results, then the second, etc., (for example, $l = l \sum_{j=1}^{4} y_{j,l}\ h$). We found the sum of the results (total) of measurements in each attempt (batch). Thus, in the first batch of measurements, j = 1 and $Y_j = Y_1$. The results Y_1^2 were calculated and noted in Excels's file in Zenodo (ANOVA data model for the current of the PV panel—https://zenodo.org/records/15113282, accessed on 3 April 2025).

Table 1. Measurement results.

№	Photocurrent (mA)	LED Frequency (Hz)	Title Group	Illumination (Lk)
1	10.0	20	Low (20–60)	1425
2	10.3	30	Low (20–60)	2022
3	10.2	40	Low (20–60)	3073
4	10.5	50	Low (20–60)	3712
5	10.4	60	Low (20–60)	3837

Table 1. *Cont.*

№	Photocurrent (mA)	LED Frequency (Hz)	Title Group	Illumination (Lk)
6	10.6	70	Middle–Low (70–110)	3962
7	10.8	80	Middle–Low (70–110)	4954
8	10.6	90	Middle–Low (70–110)	3944
9	10.4	100	Middle–Low (70–110)	3823
10	10.3	110	Middle–Low (70–110)	3680
11	10.4	120	Middle–High (120–180)	3641
12	10.2	130	Middle–High (120–180)	3583
13	10.4	150	Middle–High (120–180)	3510
14	10.3	170	Middle–High (120–180)	3498
15	10.1	180	Middle–High (120–180)	3425
16	9.30	190	High (190–220)	3367
17	8.9	200	High (190–220)	3266
18	7.9	210	High (190–220)	3030
19	7.4	220	High (190–220)	2950
20	7.8	210	High (190–220)	3040
21	7.6	220	High (190–220)	2970
22	7.4	220	High (190–220)	2950
23	7.2	220	High (190–220)	2970
24	7.3	220	High (190–220)	2940

We divided the results obtained (for each batch):

$$\frac{1}{m_j} Y_j^2 = \frac{1}{m_l} Y_l^2. \tag{6}$$

The sums of the squared measurement results for each batch were calculated separately. For the first batch,

$$\sum_{l=1}^{m_j} y_{j,l}^2 = \sum_{l=1}^{m_1} y_{1,l}^2 \tag{7}$$

The calculation of the sum results of all the measurements was as follows:

$$\sum_{j=1}^{m} Y_j = \sum_{j=1}^{4} Y_j = \sum_{j=1}^{u} \sum_{l=1}^{m} y_{jl} \tag{8}$$

We found the sum of the squared results of all the measurements as follows:

$$Q_2 = \sum_{j=1}^{u} \frac{Y_j^2}{m_j} \tag{9}$$

We found the sum of the sum of the squared results of all the measurements as follows:

$$Q_1 = \sum_{j=1}^{u} \sum l = 1 m_j y_j, l^2 \tag{10}$$

We found the total number of measurements M. For the calculation of the overall average for all the measurements, the square of the total was divided by the number of all the observations, as follows:

$$Q_3 = \frac{1}{M} (\sum_{j=1}^{u} Y_j)^2 \tag{11}$$

The total sum of the squared deviations was calculated as follows:

$$S = Q_1 - Q_3 \tag{12}$$

The i_{um} of the squared deviations in the middle of the series was calculated as follows:

$$S_0 = Q_1 - Q_2 \tag{13}$$

The sum of the squared deviations between the measurement series was calculated as follows:

$$S_x = Q_2 - Q_3 = S - S_0 \tag{14}$$

The number of batches (series of measurements) u = 4. The number of degrees of freedom in the middle of the series was $\nu_0 = M - u$. The number of degrees of freedom between the series was $\nu_x = u - 1$. The total number of degrees of freedom was $\nu = M - 1$. The total sample variance was calculated as follows:

$$S_2 = \frac{S}{\nu_2} \tag{15}$$

The sample variance in the middle of the series was calculated as follows:

$$S_{02} = \frac{S_0}{\nu_0} \tag{16}$$

The sample variance between series was calculated as follows:

$$S_{x2} = \frac{S_x}{\nu_x} \tag{17}$$

We checked the significance of the influence of factor x, for which we found the variance ratio (the calculated value of the Fisher's criterion):

$$F = \frac{S_x^2}{S_0^2} \tag{18}$$

The range of illumination frequencies (20 Hz to 220 Hz) was selected to simulate common real-world pulse-width modulated (PWM) LED sources, including those typically found in low-cost or improvised lighting scenarios during wartime and emergency conditions. Frequencies below 60 Hz were chosen to capture the effects of visible flicker, while those above 100 Hz represented conditions where flicker was imperceptible to the human eye but might still influence the photovoltaic response. The selected range also spanned the transition from significant light cycling (20–60 Hz) to quasi-continuous illumination

(>200 Hz), enabling an analysis of how the electrical response of the panel correlated with the varying rates of change in irradiance.

3. Results

3.1. Investigation of the Shading Effects

It is important to analyze shading effects. For this purpose, it is better to use larger panels and specifically change the area under shade. This test enables students to understand the negative influence of shading and analyze the VA characteristics. The VA characteristics obtained are presented in Figure 12.

Figure 12 presents the IV characteristics of the PV module under four distinct shading conditions: no shading (0%), slight shading (10% panel coverage), slight shading (20% panel coverage), moderate shading (40%). Shading was created artificially, i.e., a certain part of the module was covered with a non-transparent material. Quantitative analysis demonstrated significant reductions in photovoltaic performance as the shading increased:

- under slight shading (20%), the maximum power P_{max} decreased by approximately 22%, with V_{oc} relatively unaffected and I_{sc} dropping by approximately 20%. The fill factor reduced slightly from 0.75 (unshaded) to 0.71;
- under moderate shading (40%), the maximum power P_{max} dropped by approximately 48%. This was primarily due to a significant decrease in I_{sc} (45%) and a minor decrease in V_{oc}. The fill factor also declined to approximately 0.65.

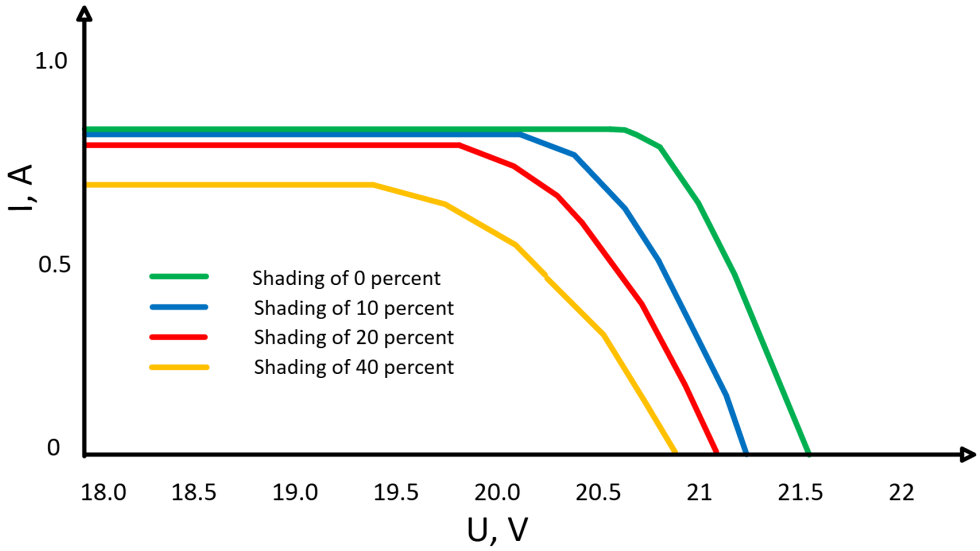


Figure 12. VA characteristics for analyzed PV module for different shadings.

This analysis clearly underscores that even partial shading considerably impacts photovoltaic performance, dramatically reducing efficiency. In practical terms, these findings highlight the critical importance of minimizing shading or integrating bypass diode systems in photovoltaic installations, particularly in environments where shading from debris or structural obstacles is frequent, such as wartime conditions.

3.2. Investigation of the Frequency of the LED Backlighting of a Photovoltaic Panel

During the operation of photovoltaic panels (PVs) their generation decreases because of short-term interference with the passage of sunlight to the PV. We propose using the light flux from a white LED to illuminate the PV panels at this time.

We determined whether the frequency of the harmonic signal (which is supplied from the generator to the LED) affects the photocurrent of the photovoltaic module. Figure 13 shows the equipment for the study; photovoltaic panel, multimeter, luxmeter, photodiodes.

The measurement results are shown in Table 1. To assess whether differences in PV module output current across various LED frequency levels were statistically significant, a one-way analysis of variance (ANOVA) was conducted. The dependent variable was the average photocurrent (mA), and the independent variable was the frequency group (categorized into four ranges: low (20–40 Hz), medium–low (60–80 Hz), medium–high (100–140 Hz), and high (180–220 Hz)).

ANOVA was selected because it is appropriate for comparing the means of three or more independent groups when the dependent variable is continuous. The assumptions required for ANOVA include the following: (1) independence of observations (ensured by separate measurements for each frequency); (2) normal distribution of residuals (verified using Shapiro–Wilk tests for each group, $p > 0.05$); (3) homogeneity of variances (checked using Levene's test, $p = 0.128$, indicating equal variances between groups). These conditions were satisfied, validating the use of ANOVA for this dataset.

From [31,32], the F test value for the five percent significance level and the number of degrees of freedom $v_1 = v_x$ and $v_2 = v_0$ is equal to

$$F_{0.05} = 49.79$$

Since $F < F_{0.05}$, the effect of frequency on the current of the photovoltaic panel can be considered significant and, therefore, the panel should be illuminated with LEDs by applying a voltage of 80 Hz.

The portability and robustness of the developed laboratory stands were practically validated through a series of field tests in realistic operational conditions. Specifically, the equipment was repeatedly assembled, disassembled, and transported between various locations, including indoor university laboratories, outdoor sites, and temporary shelters that simulated emergency conditions. During these tests, the stands were transported by hand or vehicle, reassembled, and operationally tested within approximately 10–15 min upon arrival at each location. Performance, including sensor accuracy and data log stability, was consistently maintained throughout these transitions without the need for significant recalibration. In addition, field trials included powering the devices via portable USB power banks and laptop batteries to simulate realistic off-grid scenarios. These practical validations demonstrated the suitability and reliability of the stands for deployment in real-world wartime operational environments where flexibility, ease of setup, and power independence are crucial.



(**a**)



(**b**)



(**c**)

Figure 13. (**a**) Research equipment: panel; (**b**) source of light; (**c**) and impulse generator (low-frequency).

4. Discussion

The findings presented in this study have important practical implications for maintaining and advancing renewable energy infrastructure in Ukraine, particularly during and after the ongoing military conflict. The developed portable laboratory stands offer an immediate and scalable solution for the following:

(1) Rapid on-site diagnostics of photovoltaic installations damaged by shelling or sabotage;
(2) Supporting the decentralization of energy systems by enabling maintenance of micro- and mini-PV grids in rural and conflict-affected areas;

(3) Continuing technical education and workforce training under disrupted conditions, ensuring that future engineers and technicians retain hands-on competencies even when traditional laboratories are inaccessible.

Specifically, the shading experiment results highlight the urgent need to rapidly detect and mitigate partial shading issues in surviving solar fields, as even 25% shading can result in a 22% loss of output, and 75% shading can reduce production by 73%. Such severe reductions are especially critical in the Ukrainian context, where maintaining every available kilowatt hour is vital for hospitals, communications, and military operations.

During the study, the effect of backlight frequency on the photocurrent generated by the photovoltaic panel (PVP) was analyzed. Data were grouped into four frequency ranges: low (20–60 Hz), medium–low (70–110 Hz), medium–high (120–180 Hz), and high (190–220 Hz) (see Table 1). For each group, photocurrent measurements were taken, followed by a one-way analysis of variance (ANOVA). The results showed the following:

- F-statistic = 49.47—indicated a significant difference between the groups.
- p-value = 1.95×10^{-9}—significantly less than the threshold value of 0.05.

This allowed us to reject the null hypothesis with a high level of statistical confidence and conclude that the backlight frequency had a statistically significant effect on the photocurrent generated by the PVP. It is particularly noteworthy that as the frequency increased to a certain optimal value (approximately 80–90 Hz), the photocurrent increased, after which a gradual decrease was observed. This indicates a non-linear relationship between backlight frequency and photocurrent, which should be considered when designing systems for leveling the daily generation schedules of PVPs.

The peak photocurrent observed around 70–80 Hz suggests that this frequency range offers a balance between minimizing flicker-induced energy loss and avoiding the onset of LED driver limitations at higher frequencies. Beyond 100–120 Hz, the decrease in current may be attributed to the reduced luminous efficiency of LEDs and the finite response time of the PV cell to rapid irradiance oscillations. Therefore, 80 Hz was selected as the recommended operational frequency due to its empirical performance and practical feasibility.

The successful portability validation of the systems shows that diagnostic efforts do not need centralized labs, which may be destroyed or inaccessible during active conflict. Instead, small teams can be equipped with these mobile units to perform urgent field diagnostics, reducing system downtime and enabling faster renewable energy recovery and resilience-building efforts, a strategic priority outlined in the Ukraine Renewable Energy Action Plan and supported by international recovery frameworks such as the G7+ Ukraine Energy Coordination Group.

Thus, the developed systems directly contribute to strengthening Ukraine's energy security, building local technical capacity, and supporting the ongoing transition towards decentralized, resilient, renewable energy systems that are essential both during wartime and for post-war recovery.

Despite the promising results, several limitations and challenges were identified in the present study:

(1) Measurement accuracy. Although sufficient for educational and field diagnostics purposes (2–3% error), the measurement accuracy of low-cost sensors (e.g., INA219) remains inferior to that of professional-grade photovoltaic analyzers. Future work could focus on integrating higher-precision sensing modules and implementing real-time digital calibration routines to enhance accuracy;

(2) Environmental durability. Although the laboratory stands demonstrated basic portability and resilience, the systems are not yet fully weather-proofed for long-term outdoor deployment in harsh environmental conditions (e.g., heavy rain, dust, ex-

treme cold). Future prototypes should incorporate ruggedized IP-rated enclosures and shock-absorbing structural designs;

(3) Limited scalability. The current systems are optimized for single-module analysis. Scaling the system for string or array-level diagnostics would require redesigning the data-acquisition system, enhancing wireless data handling capabilities, and ensuring safety measures (e.g., higher voltage handling);

(4) Power independence. Although we demonstrated off-grid operation using portable power banks, longer-term field deployments would benefit from integrated renewable energy charging (e.g., small solar panels with battery packs) to ensure complete autonomy;

(5) Data security and remote access. In conflict conditions, secure remote data transmission is critical. Future iterations could incorporate encryption protocols and redundancy (e.g., dual data logging locally and in the cloud) to improve data resilience against communication outages or cyber threats.

Addressing these challenges will further enhance the field-readiness, precision, and strategic impact of portable photovoltaic diagnostic laboratories, particularly in wartime or disaster recovery contexts.

5. Conclusions

This work introduces and validates portable, cost-effective laboratory systems uniquely adapted to wartime conditions, offering a practical, replicable solution for preserving renewable energy research, education, and diagnostics during infrastructure crises.

These tools are not only innovative but also essential for ensuring the continuity of research in challenging environments and the preparation of new generation power engineering. The integration of advanced sensors, microcontrollers, and data-processing systems provides a comprehensive platform for the analysis of PV modules and for the study of students to learn new technologies. The results obtained highlight the importance of accurate parameter estimation and real-time monitoring to optimize the performance and efficiency of photovoltaic systems in the Ukrainian power system operating under Ukrainian conditions. The study also underscores the need for continued innovation and adaptation in the face of environmental and operational challenges. In general, the research presented in this paper makes a significant contribution to the field of renewable energy, offering practical solutions to improve the resilience and effectiveness of the research of PV modules. Future studies should build on these findings, exploring new technologies and methodologies to further advance the field. The originality of the code of the tracker control program is the presence of a module that, based on the signal coming from the anemometer, commands the horizontal position of the desktop. The developed stands allow the location of research to be changed in cases of threat to the life of researchers during military operations or during natural disasters. The developed remote laboratory stands are in the Laboratory of "Solar Energy, Energy Storage Systems and Production Forecasting" and are used in the educational process of students specializing in specialty 145—Renewable Energy Sources and Hydropower [33,34].

Future Work

Future work will focus on several specific directions to enhance the functionality, reliability, and scalability of the proposed portable laboratory systems:

(1) Environmental ruggedization. Developing weather-proof and shock-resistant enclosures to protect sensitive electronics and ensure system operability in harsh outdoor environments, including heavy rain, dust storms, and freezing temperatures;

(2) Expanded sensing capabilities. Integrating additional sensors for irradiance, panel temperature, and ambient environmental conditions to enable a more accurate normalization of photovoltaic performance metrics to standard testing conditions (STCs);
(3) Multi-module and string-level testing. Extending the system's capabilities to support diagnostics of photovoltaic module strings (series-connected panels) through higher voltage handling and enhanced data-acquisition modules;
(4) Energy autonomy. Incorporating renewable-powered charging systems (e.g., small integrated solar panels with energy storage) to enable fully autonomous off-grid field operations without dependence on external battery packs or generators;
(5) Secure wireless data transmission. Implementing encryption and redundant cloud storage features to ensure secure and resilient remote data monitoring under the unstable communication conditions commonly encountered in wartime zones;
(6) Field validation campaigns. Conduct extended-duration field deployments at operational solar energy sites, both in Ukraine and internationally, to evaluate long-term durability, calibration stability, and user feedback in various operational contexts.

These future improvements will further optimize the systems for real-world deployment in crisis and post-crisis renewable energy recovery efforts.

Author Contributions: Conceptualization, S.B., O.R. (Oleksandr Rubanenko), A.S., I.H., M.B. and O.R. (Olena Rubanenko); methodology, O.R. (Oleksandr Rubanenko) and O.R. (Olena Rubanenko); validation, M.B., S.B., O.R. (Oleksandr Rubanenko) and A.S.; formal analysis, M.B., O.R. (Oleksandr Rubanenko) and O.R. (Olena Rubanenko); investigation, I.H., M.B., O.R. (Oleksandr Rubanenko) and O.R. (Olena Rubanenko); resources, I.H., M.B., O.R. (Oleksandr Rubanenko) and O.R. (Olena Rubanenko); writing—original draft preparation, A.S., M.B. and O.R. (Olena Rubanenko); writing—review and editing, S.B., O.R. (Oleksandr Rubanenko), A.S., I.H., M.B. and O.R. (Olena Rubanenko). All authors have read and agreed to the published version of the manuscript.

Funding: These results were supported by projects 25-PKVV-UM-001, 25-PKVV-003 and MSCA4Ukraine ID number 1233365.

Data Availability Statement: Most data are included in the article. Additional information and data are available from the corresponding author if required.

Acknowledgments: We want to thank the University of West Bohemia in Pilsen, Vinnytsia National Technical University, Institute of Renewable energy NAS Ukraine for all-round support in this research work.

Conflicts of Interest: The authors declare no conflicts of interest.

Appendix A. Arduino Code for Sensor and Communication

Listing A1. ESP8266 Sensor and Communication Code.

```
#include <Arduino.h>
#include <ESP8266WiFi.h>
#include <ESP8266HTTPClient.h>
#include <EEPROM.h>
#define EEPROM_SIZE~12

int redPin = D8;
int greenPin = D7;
char WIFI_SSID[32] = "solar";
char WIFI_PASSWORD[32] = "admin";
char URL[64] = "http://dns_of_server/api.php";

char wifi_ssid_private[32];
char wifi_password_private[32];
char clientName[10] = "1000001";
```

```
char ipAddr[64] = "http://dns_of_server/api.php";
String rezim = "normal";

int incomingByte = 0;
WiFiClient client;
HTTPClient httpClient;
String readfromport_st;

void writeEEPROM(int startAdr, int laenge, char* writeString) {
  EEPROM.begin(512);
  yield();
  for (int i = 0; i < laenge; i++) {
    EEPROM.write(startAdr + i, writeString[i]);
  }
  EEPROM.commit();
  EEPROM.end();
}

void readEEPROM(int startAdr, int maxLength, char* dest) {
  EEPROM.begin(512);
  delay(10);
  for (int i = 0; i < maxLength; i++) {
    dest[i] = char(EEPROM.read(startAdr + i));
  }
  EEPROM.end();
}

void setup() {
  Serial.begin(2400);
  pinMode(redPin, OUTPUT);
  pinMode(greenPin, OUTPUT);
  digitalWrite(greenPin, LOW);
  digitalWrite(redPin, LOW);
  delay(100);

  readEEPROM(0, 32, wifi_ssid_private);
  readEEPROM(32, 32, wifi_password_private);
  readEEPROM(64, 10, clientName);
  readEEPROM(74, 16, ipAddr);

  WiFi.begin(wifi_ssid_private, wifi_password_private);
  int count = 0;
  while (WiFi.status() != WL_CONNECTED && count < 20) {
    delay(500);
    count++;
  }

  if (count > 18) {
    digitalWrite(redPin, HIGH);
    WiFi.begin(WIFI_SSID, WIFI_PASSWORD);
    while (WiFi.status() != WL_CONNECTED) {
      delay(500);
    }
    rezim = "rezerv";
  }
}

void loop() {
  while (Serial.available()) {
    readfromport_st = Serial.readString();
    if (rezim == "normal") {
      String data = "mak=" + String(clientName) + "&name=dataset&value=" +
          readfromport_st;
```

```
      httpClient.begin(client, URL);
      httpClient.addHeader("Content-Type", "application/x-www-form-
          urlencoded");
      httpClient.POST(data);
      String content = httpClient.getString();
      httpClient.end();
      String speed = content.substring(4, content.length());
      Serial.println(speed);
    } else {
      String data = "mak=" + String(clientName) + "&name=newsid&value=0";
      httpClient.begin(client, URL);
      httpClient.addHeader("Content-Type", "application/x-www-form-
          urlencoded");
      httpClient.POST(data);
      String content = httpClient.getString();
      httpClient.end();
      int pos = content.indexOf("===");
      int pos1 = content.indexOf("---");
      String login = content.substring(4, pos);
      String pas = content.substring(pos + 3, pos1);
      Serial.println("15000");
      char char_array1[32];
      char char_array2[32];
      login.toCharArray(char_array1, login.length() + 1);
      pas.toCharArray(char_array2, pas.length() + 1);
      writeEEPROM(0, 32, char_array1);
      writeEEPROM(32, 32, char_array2);
      digitalWrite(redPin, LOW);
      digitalWrite(greenPin, HIGH);
    }
  }
}
```

Appendix B. Arduino Code for Solar Tracker

Listing A2. Solar Tracker Code for DS18B20 and LDR-driven Servo Movement.

```
#include <Servo.h>
#include <DS18B20.h>
DS18B20 ds(7); // DS18B20 on pin~7

int mode = 0, axe = 0;
int buttonState1 = 0, buttonState2 = 0;
int prevButtonState1 = 0, prevButtonState2 = 0;

int ldrtop = 0, ldrright = 1, ldrleft = 2, ldrbot = 3;
int top = 0, bot = 0, left = 0, right = 0;
int threshold_value = 10;

Servo servo_updown;
Servo servo_rightleft;

void setup() {
  Serial.begin(9600);
  Serial.println("CLEARDATA");
  Serial.println("LABEL,t,voltage,temperature,Mode");

  pinMode(12, INPUT);  // Mode switch
  pinMode(11, INPUT);  // Axis switch
  pinMode(A4, INPUT);  // Potentiometer
  pinMode(8, INPUT);   // Wind~limit

  servo_updown.attach(5);
```

```
  servo_rightleft.attach(6);
}

void loop() {
  float volt = analogRead(A5) * 5.0 / 1023;
  float voltage = volt;
  float current = voltage / 20;
  float power = voltage * current;
  float t = 0; // ds.getTempC();
  Serial.print("DATA,TIME,");
  Serial.print(voltage); Serial.print(",");
  Serial.print(t); Serial.print(",");

  buttonState1 = digitalRead(12);
  if (buttonState1 != prevButtonState1) {
    if (buttonState1 == LOW) mode = 1 - mode;
  }
  prevButtonState1 = buttonState1;
  delay(50);

  if (mode == 0) {
    Serial.println('M');
    manualsolartracker();
  } else {
    Serial.println('A');
    automaticsolartracker();
  }
}

void automaticsolartracker() {
  top = analogRead(ldrtop);
  bot = analogRead(ldrbot);
  left = analogRead(ldrleft);
  right = analogRead(ldrright);

  int diffelev = top - bot;
  int diffazi = right - left;

  if (digitalRead(8) == 0) {
    if (abs(diffazi) >= threshold_value) {
      if (right > left && servo_rightleft.read() < 180)
        servo_rightleft.write(servo_rightleft.read() + 1);
      if (right < left && servo_rightleft.read() > 0)
        servo_rightleft.write(servo_rightleft.read() - 1);
    }

    if (abs(diffelev) >= threshold_value) {
      if (top > bot && servo_updown.read() < 180)
        servo_updown.write(servo_updown.read() - 1);
      if (top < bot && servo_updown.read() > 0)
        servo_updown.write(servo_updown.read() + 1);
    }
  } else {
    servo_updown.write(80);
    servo_rightleft.write(90);
  }
}

void manualsolartracker() {
  buttonState2 = digitalRead(11);
  if (buttonState2 != prevButtonState2) {
    if (buttonState2 == LOW) axe = 1 - axe;
  }
```

```
  prevButtonState2 = buttonState2;
  delay(50);

  if (axe == 0)
    servo_rightleft.write(map(analogRead(A4), 0, 1023, 0, 180));
  else
    servo_updown.write(map(analogRead(A4), 0, 1023, 0, 180));
}
```

References

1. Cleary, K.; Palmer, K. *Renewables 101: Integrating Renewable Energy Resources into the Grid*; Resources for the Future: 2020. Available online: https://www.rff.org/publications/explainers/renewables-101-integrating-renewable-energy-resources-grid/ (accessed on 18 April 2024).
2. Belik, M.; Rubanenko, O. Implementation of Digital Twin for Increasing Efficiency of Renewable Energy Sources. *Energies* **2023**, *16*, 4787. [CrossRef]
3. Passage of the Autumn-Winter Periods of 2022–2024. State of the Power System. 18 April 2024. Available online: https://www.irf.ua/prohodzhennya-osinno-zymovyh-periodiv-2022-2024-rr-stan-energosystemy/ (accessed on 18 April 2024).
4. Russia's War on Ukraine: Implications for EU Energy Supply. European Union, 2022. Available online: https://www.europarl.europa.eu/RegData/etudes/ATAG/2022/729281/EPRS_ATA(2022)729281_EN.pdf (accessed on 18 April 2024).
5. Galushchenko, G. 50% of Ukraine's Energy Infrastructure Has Been Damaged. United for Justice Conference, Lviv, 2022. Available online: https://www.kmu.gov.ua/en/news/poshkodzheni-50enerhetychnoi-infrastruktury-ukrainy-rosiia-maie-vidpovistyza-tse-herman-halushchenko (accessed on 18 April 2024).
6. Draft Ukraine Recovery Plan: Materials of the "Audit of War Damage", 2022. Available online: https://uploadsssl.webflow.com/621f88db25fbf24758792dd8/62c48b51bd97677a3c4d7b1c_Audit%20of%20war%20damage.pdf (accessed on 18 April 2024).
7. Ukrenergo Showed a Transformer Hit by a Russian Missile. Available online: https://www.unian.ua/economics/energetics/viyna-v-ukrajini-v-ukrenergo-pokazali-transformator-v-yakiy-vluchila-rosiyska-raketa-12048951.html (accessed on 18 April 2024).
8. Trunova, I.; Miroshnyk, O.; Ladyzhynskii, I.; Moroz, O.; Onegina, V.; Qawaqzeh, M. The Motivational Model for Improvement of Electricity Supply Continuity in Post-War Ukraine. In Proceedings of the 2023 IEEE 4th KhPI Week on Advanced Technology (KhPIWeek), Kharkiv, Ukraine, 2–6 October 2023; pp. 1–6. [CrossRef]
9. Mohsin, M.; Saqib, S. Harnessing Renewable Energy for a Sustainable Future. In *Energy Crisis and Its Impact on Global Business*; IGI Global: Hershey, PA, USA, 2024; pp. 133–148.
10. Moe, E. *Renewable Energy Handbook of the Anthropocene: Humans Between Heritage and Future*; Springer International Publishing: Lexington, MA, USA, 2023 ; pp. 285–289.
11. Kendrick, G.C. Sustainability Aspects of Large-Scale Wind Power Development. In *Infrastructure Sustainability and Design*; Routledge: Abingdon, UK, 2013; pp. 103–119.
12. Algarni, S.; Tirth, V.; Alqahtani, T.; Alshehery, S.; Kshirsagar, P. Contribution of Renewable Energy Sources to the Environmental Impacts and Economic Benefits for Sustainable Development. *Sustain. Energy Technol. Assess.* **2023**, *56*, 103098. [CrossRef]
13. Goswami, Y. A Quiet Revolution is About to Take Place. *Refocus* **2004**, *5*, 21. [CrossRef]
14. Aswathanarayana, U.; Harikrishnan, T.; Kadher-Mohien, T.S. (Eds.) *Green Energy*; CRC Press: Boca Raton, FL, USA, 2010.
15. Racine, T.; Kobinger, G.P. Challenges and Perspectives on the Use of Mobile Laboratories During Outbreaks and Their Use for Vaccine Evaluation. *Hum. Vaccines Immunother.* **2019**, *15*, 2264–2268. [CrossRef] [PubMed]
16. Franzblau, C.; Romney, C.A.; Faux, R.; DeRosa, D. Mobile Laboratory Programs as Vehicles to Promote STEM Education in K-12 and Beyond. In Proceedings of the 2011 Frontiers in Education Conference (FIE), Rapid City, SD, USA, 12–15 October 2011; pp. T3D-1–T3D-6.
17. Mushasha, R.; Paez Jimenez, A.; Dolmazon, V.; Baumann, J.; Jansen, A.; Storozhenko, O.N.; El-Bcheraoui, C. Existing Operational Standards for Field Deployments of Rapid Response Mobile Laboratories: A Scoping Review. *Front. Public Health* **2024**, *12*. [CrossRef] [PubMed]
18. Vorobyev, A.I.; Gavrilyuk, M.V.; Vorobyeva, T.V.; Morozov, D.Y.; Merkovich, A.M. Scientific Approaches to the Identification of Test Objects and Types of Tests for Mobile Research Laboratories in the Field of Intelligent Transport Systems. In Proceedings of the 2024 Systems of Signals Generating and Processing in the Field of on Board Communications, Moscow, Russian, 12–14 March 2024; pp. 1–4.
19. Schneider, B.; Schüle, S.; Kürümlüoglu, M.; Riedel, O. Mobiles Plug-In Labor. *Z. Wirtsch. Fabrikbetr.* **2021**, *116*, 75–81. [CrossRef]
20. Palmiotti, E.C.; Springer, M.; Zuboy, J.; Silverman, T.J.; Braid, J.L.; Jordan, D.C.; Rabade, S.; Barnes, T.M. Growing Panes: Investigating the PV Technology Trends Behind Frequent Early Failures in Modern Glass–Glass Modules. *IEEE J. Photovoltaics* **2025**, *15*, 297–308. [CrossRef]

21. Rubanenko, O.; Belik, M.; Rubanenko, O.; Bobba, P.B.; Smaglo, I.; Lakshmi, G.S. Determining Probable Locations of Photovoltaic Modules Malfunctions. In Proceedings of the 2024 IEEE 4th International Conference on Sustainable Energy and Future Electric Transportation (SEFET), Hyderabad, India, 31 July–3 August 2024; pp. 1–6. [CrossRef]
22. Li, G.; Zhang, Y.; Zhou, H.; Guan, Y. Parameter Identification and Output Characteristics Modelling of Photovoltaic Module Based on Effective Irradiance Correction. *Trans. China Electrotech. Soc.* **2024**, *39*. [CrossRef]
23. Hao, S.; Qi, T.; Ma, X.; Li, J.; Li, T. RP-CFANet: An Adaptive Photovoltaic Hot-Spot Fault Detection Network Based on Region Perception and Cross-Channel Feature Aggregation. *IEEE Trans. Instrum. Meas.* **2025**, *74*, 3530714. [CrossRef]
24. Choi, H.; Choi, J.; Ahn, S.H.; Hyun, J.H.; Cha, H.L.; Lim, B.Y.; Ahn, H.K. Optimal Inclination and Azimuth Angles of a Photovoltaic Module With Load Patterns for Improved Power System Stability. *IEEE J. Photovoltaics* **2024**, *14*, 525–537. [CrossRef]
25. Castallà, M.; Kapouropoulos, K.; Urbano, E.; Romeral, L. Supervision and Fault Detection System for Photovoltaic Installations Based on Classification Algorithms. *Renew. Energy Power Qual. J.* **2020**, *18*, 375–379.
26. Kandeal, A.W.; Elkadeem, M.R.; Thakur, A.K.; Abdelaziz, G.B.; Sathyamurthy, R.; Kabeel, A.E.; Yang, N.; Sharshir, S.W. Infrared Thermography-Based Condition Monitoring of Solar Photovoltaic Systems: A Mini Review of Recent Advances. *Sol. Energy* **2021**, *223*, 33–43. [CrossRef]
27. Degradation of PV Modules, Inverters, Components and System. Available online: https://energy.ec.europa.eu/system/files/2022-09/degradation-of-pv-modules-inverters-components-and-system.pdf (accessed on 18 April 2024).
28. Performance Ratio—Quality Factor for the PV Plant. Available online: https://www.pv-tech.org/technical-briefing/performance-ratio-quality-factor-for-the-pv-plant/ (accessed on 18 April 2024).
29. Shimada, S.; Mizuochi, H.; Takeuchi, W. Investigation of Spectral Variations in Different Solar Photovoltaic Modules Using Spaceborne and In-Situ Hyperspectral Data. *IEEE J. Sel. Top. Appl. Earth Obs. Remote Sens.* **2025**, 18, 9701–9707. [CrossRef]
30. Belik, M.; Rubanenko, O.; Bobba, P.B. Increasing Efficiency PV System Due Considering Technical Condition. In Proceedings of the 2024 IEEE 65th International Scientific Conference Power and Electrical Engineering of Riga Technical University (RTUCON), Riga, Latvia, 10–12 October 2024; pp. 1–5. [CrossRef]
31. Plonsky, M. One Way ANOVA. Available online: https://www.uwsp.edu/psych/stat/12/anova-1w.htm (accessed on 13 November 2007).
32. Gupta, B.B.; Gaurav, A.; Chui, K.T. Robust Phishing Detection in Consumer IoT Devices with ANOVA F-Test and Satin Bowerbird Optimization of Deep Learning Model. In Proceedings of the 2025 IEEE International Conference on Consumer Electronics (ICCE), Las Vegas, NV, USA, 11–14 January 2025; pp. 1–6. [CrossRef]
33. Laboratory of "Solar Energy, Energy Storage Systems and Production Forecasting". Available online: https://iq.vntu.edu.ua/departs/index.php?id=219&mode=new_item&f=674/main/Bak_laboratorii_VDE.html (accessed on 18 April 2024).
34. Renewable Energy Laboratory Catalog. Online Flipbook. Available online: https://heyzine.com/flip-book/ba48e1f379.html (accessed on 18 April 2024).

Disclaimer/Publisher's Note: The statements, opinions and data contained in all publications are solely those of the individual author(s) and contributor(s) and not of MDPI and/or the editor(s). MDPI and/or the editor(s) disclaim responsibility for any injury to people or property resulting from any ideas, methods, instructions or products referred to in the content.